Desalination and Water Treatment
www.deswater.com

doi: 10.1080/19443994.2015.1025437

57 (2016) 8815–8825
April

Taylor & Francis
Taylor & Francis Group

Electrochemical oxidation of C.I. Acid Red 73 wastewater using Ti/SnO_2-Sb electrodes modified by carbon nanotube

Li Xu[a,b,*], Yukuan Sun[a,b], Lichao Zhang[c], Jiejing Zhang[d], Fan Wang[e]

[a]*School of Chemical Engineering and Technology, Tianjin University, Tianjin 300072, P.R. China, Tel. +86 22 27409839; Fax: +86 22 27890515; emails: xuli620@163.com (L. Xu), qdsunyukuan@163.com (Y. Sun)*
[b]*Tianjin Key Laboratory of Membrane Science and Desalination Technology, Tianjin 300072, P.R. China*
[c]*Sinopec Engineering Incorporation, Beijing 100101, P.R. China, Tel. +86 22 27409839; email: hbkjdxzlc@163.com*
[d]*School of Life Sciences, Jilin Agricultural University, Changchun 130118, P.R. China, Tel. +86 431 84533360; email: zjjx124@163.com*
[e]*School of Chemical Engineering, China University of Petroleum, Beijing 102249, P.R. China, Tel. +86 10 89733288; email: tjuwangfan@gmail.com*

Received 13 September 2014; Accepted 24 February 2015

ABSTRACT

Electrochemical oxidation of C.I. Acid Red 73 (AR 73) in aqueous solution is performed in an undivided cell using Ti/SnO_2-Sb-CNT as anode. Cyclic voltammetric experiments suggest that electrochemical oxidation of AR 73 is totally irreversible and direct electron transfer does not occur on anode surface. The influence of operating parameters on the degradation efficiency is investigated systematically, including current density (25–100 mA cm^{-2}), initial dye concentration (0.5–1.5 g L^{-1}), initial pH (3–11), and different kinds of supporting electrolyte. The electrochemical degradation of AR 73 follows pseudo-first-order kinetics. The removal efficiency of AR 73 degradation increases from 78.3 to 95.7% with increased current density from 25 to 100 mA cm^{-2}. The initial AR 73 concentration has a negative effect on degradation rates at higher value, and pH has no obvious effect on the dye removal rate. The comparative experiments using Na_2SO_4, NaCl, and Na_3PO_4 as supporting electrolyte indicate that NaCl has the most significant effect on AR 73 degradation, but shows poor mineralization ability with only 51.5% removal rate of total organic carbon. The electrogenerated oxidant $S_2O_8^{2-}$ using Na_2SO_4 supporting electrolyte also contributes the dye degradation and mineralization compared with Na_3PO_4. Samples during the electrochemical oxidation process are characterized with UV–vis spectra and high performance liquid chromatography. The results show that the AR 73 and intermediates formed during the degradation are both completely removed after 3 h electrochemical oxidation. The electrochemical technique is expected to be an interesting alternative for the treatment of azo dye in wastewater.

Keywords: Electrochemical oxidation; Azo dye; SnO_2-Sb-CNT electrodes; C.I. Acid Red 73

---

*Corresponding author.

1. Introduction

Nowadays, due to the large-scale production and extensive application, large number of synthetic dyes are discharged into the aquatic ecosystem without sufficient treatment, causing considerable non-esthetic pollution and serious health problems [1–3]. Dye wastewaters usually present high stability, high levels of chemical oxygen demand (COD), and resistance to microbial attack. Therefore, the technology for decolourization and degradation of dye wastewater has been widely concerned by scientists and engineers [4–6].

Lots of wastewater treatment methods are developed to decolorize and degrade dyeing wastewater to decrease their environmental impact, such as microbiological treatments [7], enzymatic process [8], adsorption [9], membrane separation [10], ozonation [11], advanced oxidation processes (AOPs) [12,13], and photocatalysis [14]. Conventional methods such as microbiological oxidation, adsorption, and coagulation–flocculation have been extensively investigated for treating textile effluents and exhibit certain advantages, but hardly achieve complete decontamination to meet the more stringent environmental legislation [15].

Electrochemical oxidation, as one kind of AOP, has been used for the degradation of various types of textile dyes effluents. This method is a promising technology due to stable high efficiency, no production of sludge, amenability to automation, and environmental compatibility [16–18]. The hydroxyl radical (·OH) with $E^{\circ}(HO\cdot/H_2O) = 2.8$ eV/NHE generating in the electrochemical process, as a strong oxygen-based oxidizer, can non-selectively attack most dyestuff until their total mineralization into carbon dioxide, water, and inorganic ions [19]. Electrode materials is crucial for electrochemical oxidation, and different kinds of anode materials have been investigated in the last two decades, including Pt [20], glassy carbon [21], graphite [22], PbO_2 [23–25], SnO_2 [26–31], boron-doped diamond (BDD) [32–34], etc. The BDD electrode possesses high oxygen evolution potential, high current efficiency, remarkable corrosion stability, low adsorption properties, and extremely wide potential window in aqueous medium. However, the BDD anode has a larger resistance than noble metal and metal oxide electrodes [34]. In addition, the complication and high cost of preparing BDD limit its application in industry widely. The SnO_2 electrode has recently received a great deal of attention because of high electro-catalytic activity, good electrical conductivity, and low cost [28,31]. Besides, our previous research indicates that the Ti-substrate SnO_2-Sb anode modified by carbon nanotube has longer service lifetime and oxygen evolution potential [35]. The SnO_2 electrode is classed as a non-active anode. In SnO_2 electrochemical oxidation process, organics (*R*) contained in polluted solution are oxidized by direct electron transfer on the surface of anode, or rather totally mineralized with physically adsorbed hydroxyl radical ($SnO_2[\cdot OH]$) as follows [19]:

$$SnO_2 + H_2O \rightarrow SnO_2[\cdot OH] + H^+ + e^- \quad (1)$$

$$SnO_2[\cdot OH] + R \rightarrow SnO_2 + CO_2 + H_2O + H^+ + e^- \quad (2)$$

$$SnO_2[\cdot OH] + H_2O \rightarrow SnO_2 + O_2 + 3H^+ + 3e^- \quad (3)$$

The first step is the oxidation of water molecules leading to the formation of adsorbed hydroxyl radicals, which are absorbed on the active sites of the electrode surface. Then, the absorbed radical with high oxidation potential oxidizes the organic matter, which competes with the side reaction of hydroxyl radicals to oxygen.

Azo dyes, about 70% of the world dye production, are extensively used in the textile industries. Azo bonds (–N=N–) as chromophore group in association with aromatic structures make this dyestuff cause considerable non-esthetic pollution and serious health risk factors [36,37]. In this paper, the goal is to evaluate the applicability of electrochemical degradation of azo dye in aqueous solution on the Ti/SnO_2-Sb-CNT electrode using C.I. Acid Red 73 (AR 73) as a representative dye. To the best of our knowledge, there is no systematic study on the electrochemical oxidation of C.I. AR 73. In this study, the electrochemical behavior of the anode in AR 73 solution was studied by cyclic voltammetry. The effect of operating parameters, including current density, initial dye concentration, initial pH, and the type of supporting electrolyte, was investigated systematically, in order to identify the optimal electrochemical conditions which give low-energy requirements and high degradation efficiency [38]. Also, the degradation process and intermediates were monitored by UV–vis spectroscopy and chromatographic techniques.

2. Experimental

2.1. Reagents

All of the chemicals were of analytical grade and were used without further purification. Solutions were prepared using deionized Milli-Q water. C.I. AR 73 (>99% purity) was purchased from Qingdao Chuanlin

Table 1
Characteristics of C.I. AR 73

Characteristics	C.I. AR 73
Molecular formula	$C_{22}H_{14}N_4Na_2O_7S_2$
Molecular weight	556.490
λ_{max} (nm)	518
CAS number	5413-75-2
Color index number	27290
Molar volumes (mM^{-1})	323.5
Molecular structure	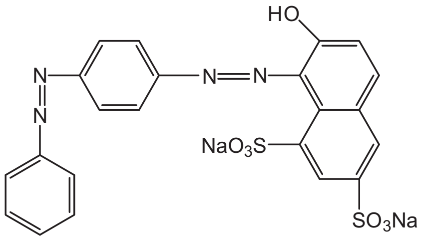
UV spectra	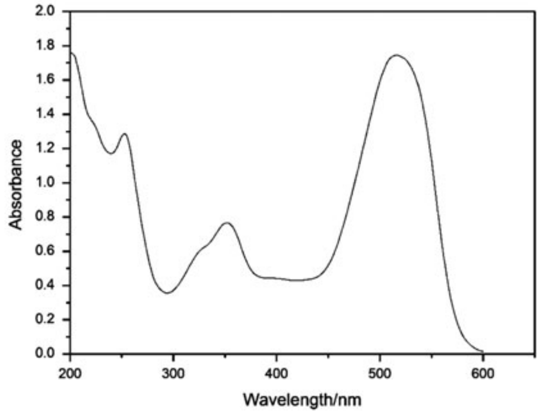

Dyestuffs Co., Ltd, Shandong, China, and its structural parameters were shown in Table 1. All the other chemicals and organic solvent were obtained from Tianjin Fuchen Chemical reagents factory, China.

2.2. Preparation of the electrodes

The detailed procedure for the preparation of the Ti/SnO_2-Sb-CNT electrode had been described in detail in our previous paper [35]. Briefly, titanium plates (99.5%, 2 cm × 2 cm × 0.5 mm) were mechanically polished with 320-grit sandpaper and degreased in 40wt.% NaOH at 90℃ for 1 h. Then, they were etched in 10 wt.% oxalic acid at 98℃ for 2 h and finally washed with double-deionized water. The SnO_2-Sb-CNT coating deposited on the pretreated titanium substrate was prepared by pulse electrodeposition method. The characterization on the surface of the Ti/SnO_2-Sb-CNT and other characterization of anode could also be found in our previous paper [33].

2.3. Electrochemical degradation of AR 73

The electrochemical degradation experiments were carried out in a one-compartment electrochemical cell with effective volume of 150 mL. The anode (Ti/SnO_2-Sb-CNT) and the cathode (titanium sheet) were positioned vertically and parallel to each other with a distance of 2 cm. The two electrodes were 8 cm^2 in area. The dye solution containing AR 73 was prepared by dissolving AR 73 in 1 L solution with 0.1 M supporting electrolyte (Na_2SO_4, or NaCl, or Na_3PO_4). The current densities of the electrochemical degradation were chosen at 25, 50, and 100 mA cm^{-2}. Different initial dye concentrations (0.5, 1.0, and 1.5 g L^{-1}) were used to examine the effect of the initial concentration on the degradation efficiency of AR 73. The pH values (3, 7, and 11) of AR 73 solution were obtained by adding an appropriate amount of H_2SO_4 or NaOH. The volume of AR 73 solution was 120 mL, and the reaction temperature was kept at 25℃ during the degradation process by a water bath [39–41]. A dc potentiostat with a voltage range of 0–30 V was employed as the power supply for AR 73 degradation studies. During the experiments, samples were drawn from the reactor at half-hour intervals and then analyzed. All of the experiments were performed in duplicate.

2.4. Analytical methods

Cyclic voltammetry was tested with a standard three-electrode cell at electrochemical workstation controlled by a computer (PARSTAT 2273, PARC, USA). The prepared Ti/SnO_2-Sb-CNT electrode was employed as a working electrode, and a platinum foil as the counter electrode. Meanwhile, the Ag/AgCl/0.1 M KCl served as the reference electrode. The exposed apparent area of the working electrode was 4 cm^2. In order to increase the reproducibility of the polarization measurements, the working electrode was electrochemically pretreated before use for 30 min in 1.0 mol/L H_2SO_4 solution under anodic current density of 50 mA cm^{-2}. The cyclic voltammetry curves were measured at 50 mV s^{-1} in 0.1 M Na_2SO_4 aqueous with or without AR 73 at temperature 25℃.

In this study, samples were selected depending on the time duration of 0, 30, 60, 90, 120, 150, and 180 min. A UV–visible spectrophotometer (UV-1000, Shanghai Tianmei scientific instruments Co., China) was used to measure the concentration and the absorbance spectra of the AR 73 solution, and all the solutions were recorded in the range of 200–600 nm. The total organic carbon (TOC) was monitored with a TOC analyzer (TOC-Vcpn, Shimadzu, Japan). The pH was determined using a pH meter (PHSJ-4F, Shanghai Leici Corporation, China). Separate experiments were run to study the main degradation products of AR 73 in the electrochemical oxidation process using a high-performance liquid chromatograph (HPLC, Ultimate 3000, America) equipped with UV detection. Aliquots of sample (e.g. 20 μL) were injected automatically into the HPLC column running with the mobile phase of acetonitrile/water (0.025 M of ammonium acetate) at 35/65 (v/v). The separation was performed using an ODS-25u reversed phase column (Alltech, USA) at a flow rate of 1 mL/min and a column temperature of 303 K. The UV detector was used with the wavelength set at 280 nm. The total analysis time was 5 min.

3. Results and discussion

3.1. Cyclic voltammetric study of AR 73 oxidation

Cyclic voltammetric experiments were performed to examine the electrochemical behavior of AR 73 at Ti/SnO_2-Sb-CNT using 0.1 M Na_2SO_4 as supporting electrolyte. The cyclic voltammograms (CVs) of the Ti/SnO_2-Sb-CNT electrode in the solution with/without AR 73 were recorded between −1.2 and 2 V, as shown in Fig. 1. It can be seen from this figure that Ti/SnO_2-Sb-CNT in blank solution and in the AR 73 solution had the similar voltammetric behaviors. There was no anodic oxidation peak appeared in the CV in the AR 73 solution compared with the CV curve recorded in the blank solution, which indicated that direct electron transfer did not occur, and the AR 73 was not directly oxidized on Ti/SnO_2-Sb-CNT but indirectly oxidized. SnO_2 anode belonged to “non-active electrodes,” [42] so the organic pollutions were mainly degraded by oxidants generated during the electro-catalytic oxidation, such as hydroxyl radical, hydrogen peroxide, and peroxydisulfate. During the cathodic sweep from 2.0 to −1.2 V, no corresponding reduction peak could be identified, suggesting that the electro-catalytic oxidation of AR 73 at Ti/SnO_2-Sb-CNT was totally irreversible.

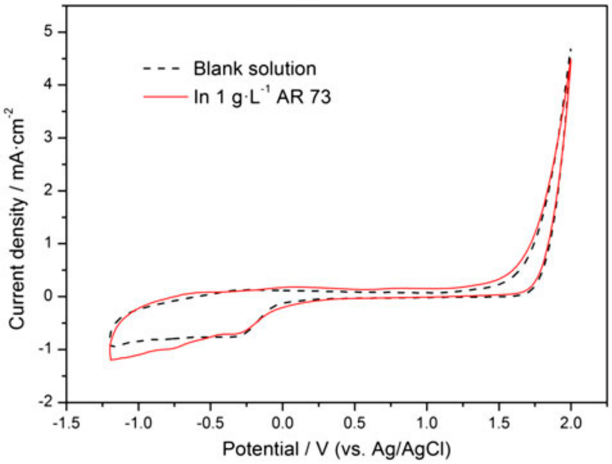

Fig. 1. Comparison of the CVs of Ti/SnO_2-Sb-CNT anode in blank 0.1 M Na_2SO_4 electrolyte and with 1.0 g L^{-1} AR 73 at scan rate 50 mV s^{-1} (initial pH 8).

In addition, the current densities in presence of AR 73 were little larger than those in the blank solution. It could be explained that H_2O was discharged on the surface of the anode to form adsorbed hydroxyl radicals [43]. When the AR 73 was added into the solution, it reacted with hydroxyl radicals, causing the diminishing of adsorbed hydroxyl radicals. Thus, the transfer of electrons on the anode surface was accelerated, resulting in the increase in calculated current density as shown in Fig. 1.

3.2. Effect of current density on AR 73 degradation

Fig. 2 shows the evolution of C/C_0 ratios (C: the residual concentration of AR 73 at a given electrolytic time, and C_0: the initial concentration of AR 73) for

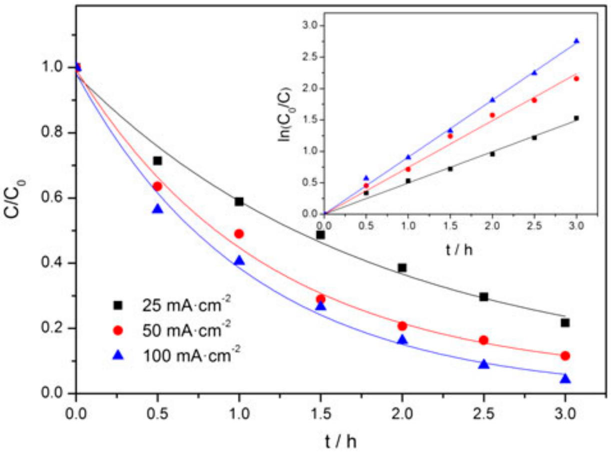

Fig. 2. Evolution of AR 73 concentration and kinetic rate constant as a function of electrolysis time in Ti/SnO_2-Sb-CNT anode cell at different current density (20, 40, and 60 mA cm^{-2}). Degradation conditions: initial concentration 1 g L^{-1}, pH (not adjusted), supporting electrolyte 0.1 M Na_2SO_4.

the electrochemical oxidation and degradation of AR 73 on the Ti/SnO_2-Sb-CNT electrode at different applied current densities (I_{appl}) (25, 50, and 100 mA cm^{-2}) in 120 mL working solution containing AR 73 concentration 1 g L^{-1} and Na_2SO_4 (0.1 M) as supporting electrolyte. After 3 h electrochemical oxidation, the degradation rate of AR 73 reached 78.3, 88.4, and 95.7%, respectively, for different current densities. The regressions of AR 73 degradation data were all linear for the three different I_{appl} values, and the electrochemical oxidation of AR 73 could be regarded as a pseudo-first-order reaction which was written as follows:

$$\frac{-\mathrm{d}[\mathrm{AR}\ 73]}{\mathrm{d}t} = k[\mathrm{AR}\ 73][\cdot\mathrm{OH}] = k_{\mathrm{app}}[\mathrm{AR}\ 73] \qquad (4)$$

The calculated apparent rate constants (k_{app}) were 0.93, 1.99, and 2.70 h^{-1} at 25, 50 and 100 mA cm^{-2}, respectively.

The removal efficiencies and degradation rates of AR 73 increased with the increase in current density. It could be explained by the fact that more electrogenerated active oxidant hydroxyl radicals (·OH) were produced on Ti/SnO_2-Sb-CNT surface from Reaction (1) at high current density. However, the larger proportion of generated ·OH was wasted by other competitive side reactions like oxygen evolution (Reaction (3)). Thus, the mass transport could be significantly increased due to the formation and detachment of O_2 bubbles, which was also explained by other authors [44,45]. So, the diffusion flux of AR 73 towards the anode surface increased with increasing the applied current density. Nevertheless, when the current exceeded a certain value, the number of active sites of the anode would be minimized because a greater amount of gas was produced at the anode surface, and the current efficiency decreased largely. It could be found that the value of k_{app} increased slightly (from 0.75 to 0.98 h^{-1}) when the I_{appl} increased from 50 to 100 mA cm^{-2}. In addition, at larger current density, the energy consumption necessary was higher and the service life of electrodes was shorted.

3.3. Effect of initial concentration on AR 73 degradation

The effect of AR 73 initial concentration on degradation was investigated at the condition of current density 50 mA cm^{-2} and supporting electrolyte Na_2SO_4 0.1 M. As observed in Fig. 3, the AR 73 removal efficiency decreased from 94.5 to 78.9% with the initial concentration of the dye increased from 0.5 to 1.5 g L^{-1}. Correspondingly, the apparent rate constants (k_{app}) decreased with the increased of initial AR 73 concentrations. The outcome was in agreement with the data reported by Lin and Niu [46]. The results could be explained by the fact that the degradation of AR 73 was mediated by hydroxyl radicals (·OH), and the ·OH generated on the surface of the anode at a given current density was identical. Thus, the electrochemical oxidation was faster than the dye

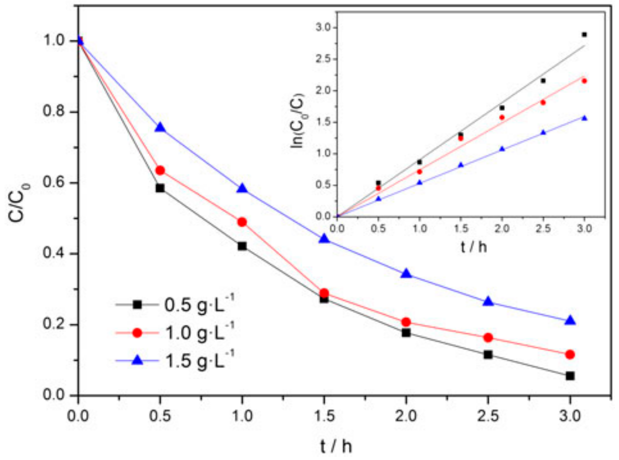

Fig. 3. Evolution of AR 73 concentration and kinetic rate constant as a function of electrolysis time in Ti/SnO_2-Sb-CNT anode cell at initial concentration (0.5, 1.0, and 1.5 g L^{-1}). Degradation conditions: current density 50 mA cm^{-2}, pH (not adjusted), and supporting electrolyte 0.1 M Na_2SO_4.

diffusion at low concentrations, resulting to the greater probability for AR 73 molecules being attacked by ·OH [47]. Hence, the value of k_{app} was relatively higher in the case. In comparison, at the high initial concentration, the surface concentration of oxidation intermediates was higher and the hydroxyl radicals had nonselective reactivity in relation to the adsorbed intermediates. That meant that part of the hydroxyl radicals were used to oxidized the intermediate products, and the AR 73 molecules could not be removed fast due to the shortage of enough ·OH. It should be pointed out that the increase in initial concentration of dye increased its concentration gradient and mass transfer across the diffusion layer, and thus its electrochemical oxidation on anode, resulting that the total amount of degraded AR 73 was greater when the initial concentration was higher.

3.4. Specific energy consumption of anodic oxidation

Table 2 shows the general current efficiency (GCE) and the specific energy consumption (SEC) under the different current density and different eye concentration.

GCE could be calculated based on Eq. (5):

$$\mathrm{GCE} = \frac{\mathrm{COD}_0 - \mathrm{COD}_t}{8It}\mathrm{FV} \tag{5}$$

where COD_t and COD_0 are the COD of AR 73 at times t and initial value (g L^{-1}), respectively. I is the current (A), F *is* the Faraday's constant, V *is* the sample volume (L).

SEC could be obtained as follows [19]:

$$\mathrm{SEC} = \frac{IUt}{(\mathrm{COD}_0 - \mathrm{COD}_t)V} \tag{6}$$

Table 2
GCE and SEC of anodic oxidation under the different conditions

Operating variables		GCE (%)	SEC kWh/(kg COD)$^{-1}$
Current density (mA cm^{-2})	25	77.05	80.00
	50	47.51	134.56
	100	26.50	342.64
Dye concentration (g L^{-1})	0.5	27.94	228.78
	1.0	47.51	134.56
	1.5	54.67	121.32

where t is the electrochemical degradation time (h), U *is* the average cell voltage (V). It could be seen that increasing the current density and decreasing eye concentration could reduce the current efficiency and improve the SEC, which was in accordance with Panizza and Cerisola [19].

3.5. Effect of initial pH on AR 73 degradation

Lots of papers had reported on the effects of the solution pH on the electrochemical oxidation of organics, and the conclusions were variant in different case, including the materials of anodes and the types of organic matter [46,48–50]. The effect of pH on AR 73 degradation efficiency was determined at the different pH (3, 7, and 11), with current density 50 mA cm^{-2}, initial concentration 1.0 g L^{-1}, and supporting electrolyte $\mathrm{Na_2SO_4}$ 0.1 M. The initial pH of AR 73 solution without pH regulation was about 8.03, and then decreased quickly during electrochemical oxidation. As shown in Fig. 4(a), the initial pH value of AR 73 solution without any regulation reached 5.12 finally after 3 h degradation. So, the continuous pH regulation had to be made in the process of electrolysis by adding NaOH for the cases of pH 7 and pH 11. For the case of pH 3, the solution pH dropped slowly, so the pH regulation was unnecessary. A similar and rapid AR 73 degradation was observed in the three cases, as shown in Fig. 4(b). About 90% dye molecules were removed after 3 h electrochemical oxidation, irrespective of acidic, neutral, or alkaline reaction media. For AR 73, a kind of anionic dye, higher pH solution would lead to the form of polymeride, which was disadvantaged to the effective degradation [47]. But, on the other hand, the alkaline environment contributed to the generation of ·OH from reaction (1). Also, the AR 73 solutions with lower pH hadn't obviously higher oxidation rate. In general, the pH had no obvious effect on the dye removal rate. Hence, the pH adjustment was not necessary in the preprocessing for the degradation of AR 73 used by the electrode, and the electrochemical oxidation could work well in a wide pH range.

3.6. Effect of supporting electrolyte on AR 73 degradation

Considering that AR 73 was a kind of weak electrolyte with low conductivity, strong electrolyte should be added to promote the conductivity of AR 73 solution. In the above experiments, sodium sulfate ($\mathrm{Na_2SO_4}$) was chosen as the supporting electrolyte. It should be pointed out that the peroxodisulfates could be formed at the anode surface (Reaction 7), and they

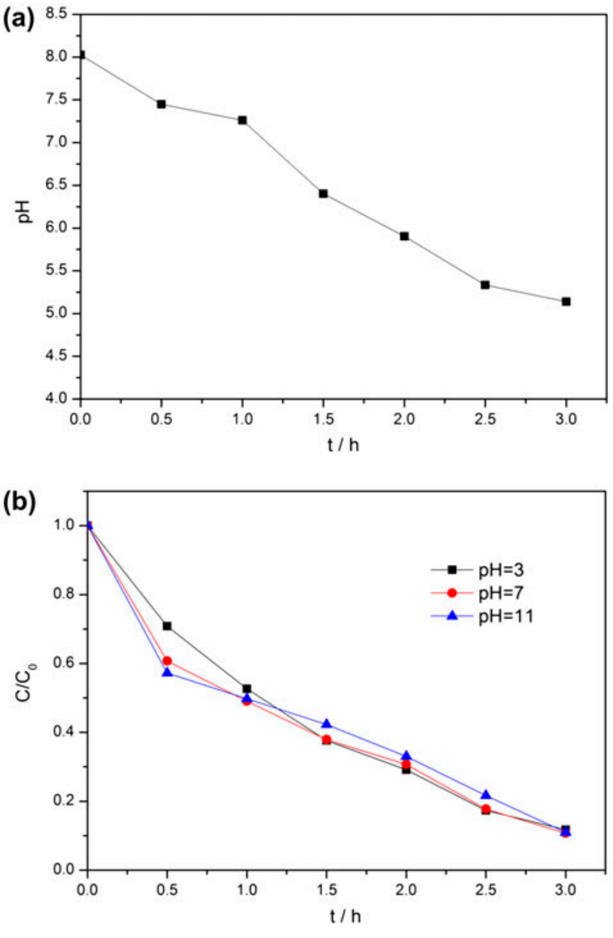

Fig. 4. Evolution of AR 73 concentration as a function of electrolysis time in Ti/SnO_2-Sb-CNT anode cell at initial pH without adjusted (a) and initial pH with adjusted (3, 7, and 11) (b). Degradation conditions: current density 50 mA cm^{-2}, initial concentration 1 g L^{-1}, supporting electrolyte 0.1 M Na_2SO_4.

were very powerful oxidant. Some paper reported the usage of the sodium chloride (NaCl) as electrolyte, because chloridion could be oxidized to active chlorine (Cl_2, HClO, and ClO^-) by reactions (8)–(10) [51,52]. Besides the direct electrooxidation by hydroxyl radicals, AR 73 might be degraded by mediated oxidation with these electrogenerated oxidants. In order to determine the role of these electrogenerated oxidants, the degradation of AR 73 using sodium phosphate (Na_3PO_4) was conducted since no electrogenerated oxidants were form in the whole process of electrochemical oxidation. Fig. 5(a) and (b), respectively, showed the evolution of AR 73 solute concentration and TOC as a function of electrolysis time in supporting media (0.1 M Na_2SO_4, 0.1 M NaCl, or 0.1 M Na_3PO_4), with current density 50 mA cm^{-2} and initial concentration 1.0 g L^{-1}.

The graph showed that the decease of dye concentration in the presence of NaCl was more rapid than the presence of Na_2SO_4 or Na_3PO_4. The generated active chlorides (Cl_2, HClO, and ClO^-) had a significant role in the AR 73 removal. However, the standard reduction potential values of these active chlorides were much lower than that of hydroxyl radical [53]. Hence, the active chlorides were not effective enough for the TOC removal and showed poor mineralization ability, as shown in Fig. 4(b). Moreover, the Cl_2 would be expected to interact with AR 73 to form stable chlorinated organic intermediates, which was refractory in nature and probably carcinogenic [54]. Compared with the case of using Na_3PO_4, the TOC removal rate increased by about 8% when Na_2SO_4 was used as supporting electrolyte. The result

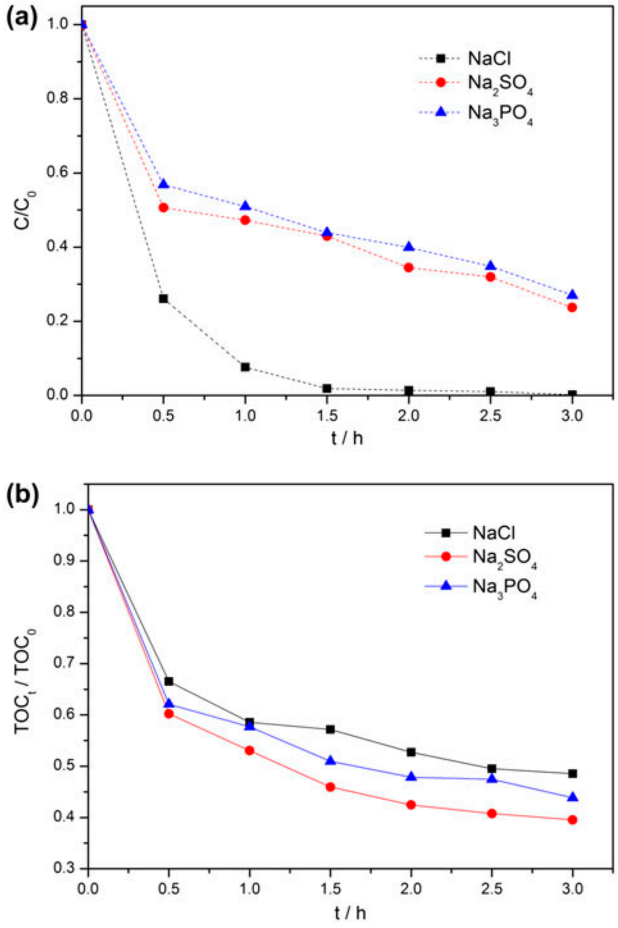

Fig. 5. Evolution of AR 73 concentration (a) and TOC (b) as a function of electrolysis time in Ti/SnO_2-Sb-CNT anode cell at different kinds of supporting electrolyte (0.1 M Na_2SO_4, NaCl, and Na_3PO_4). Degradation conditions: current density 50 mA cm^{-2}, initial concentration 1 g L^{-1}, pH (not adjusted).

indicated that the electrogenerated oxidant $S_2O_8^{2-}$ played a relative important role in the rate of mineralization in the process of treating dye wastewater.

Through the research of electrolytes, sodium sulfate was found to be the most appropriate supporting electrolyte.

$$2SO_4^{2-} \rightarrow S_2O_8^{2-} + 2e^- \tag{7}$$

$$2Cl^- = Cl_2 + 2e^- \tag{8}$$

$$Cl_2 + H_2O = HClO + H^+ + Cl^- \tag{9}$$

$$HClO = H^+ + OCl^- \tag{10}$$

3.7. UV–vis Spectrum

Fig. 6 shows the UV–vis spectral changes of AR 73 solution during electrochemical oxidation using the Ti/SnO_2-Sb-CNT electrode under the optimal conditions. The original UV–vis absorption peaks of initial AR 73 solution mainly consist of three peaks at 208, 354, 522 nm, and they are, respectively, ascribed to the presence of benzene ring, naphthalene rings, and azo linkage (chromophore) in the AR 73 molecule [55]. During the degradation process, the three absorption bands at 208, 354, and 522 nm were diminished steadily with increase in the reaction time. However, the absorbance at 290–300 nm of the solution increased after 30 min reaction compared with the before reaction and decreased to nearly zero after 180 min reaction, which might be due to the presence of the intermediate products derived from AR 73 [56]. Though the formation of intermediates could not be avoided, all of the peaks nearly disappeared, meaning the occurrence of the aromatic rings' cleavage. So the Ti/SnO_2-Sb-CNT electrode is effective for AR 73 degradation. In order to better understand the process of electrochemical oxidation using Ti/SnO_2-Sb-CNT, the changes of the HPLC chromatograms of AR 73 and intermediates at various time periods (0, 30, 90, and 180 min) are shown in Fig. 7. Fig. 7(a) shows the changes of the HPLC chromatograms of AR 73 at time

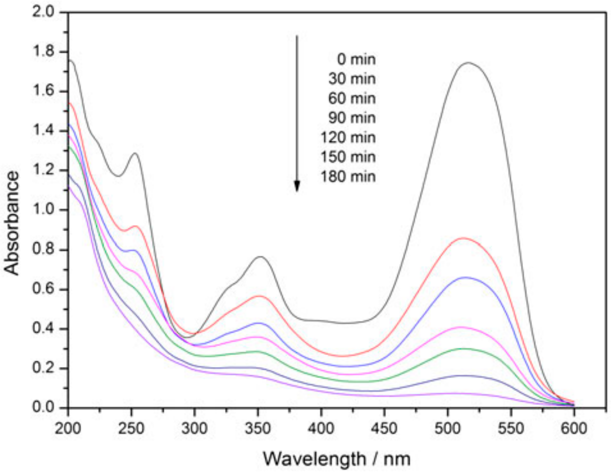

Fig. 6. UV–vis spectral changes of AR 73 solution at different electrolysis time (0, 30, 60, 90, 120, 150, and 180 min) during the electrochemical degradation process on Ti/SnO_2-Sb-CNT. Conditions: current density 50 mA cm^{-2}, initial concentration 1 g L^{-1}, pH (not adjusted), supporting electrolyte 0.1 M Na_2SO_4.

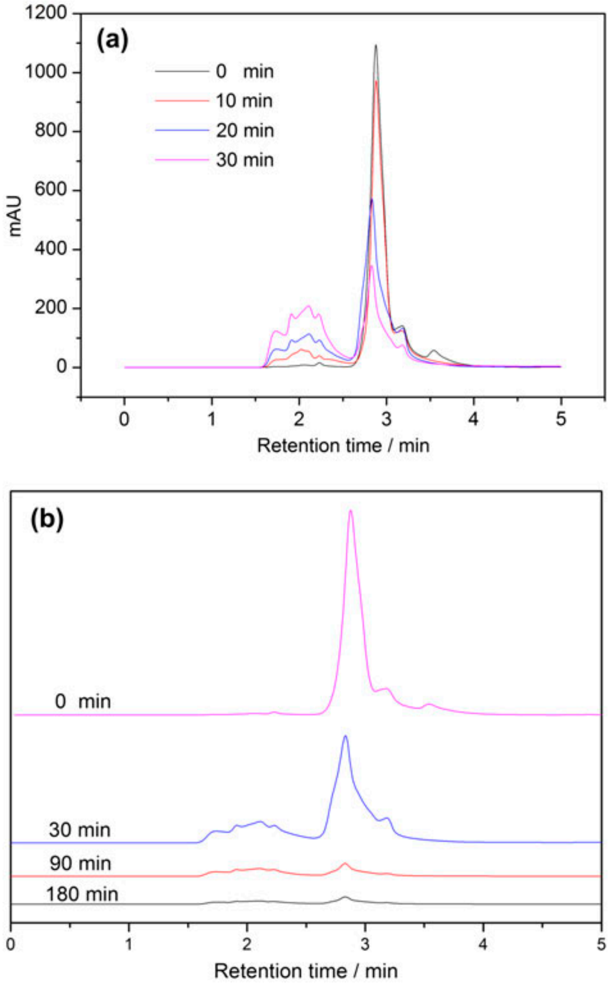

Fig. 7. The HPLC chromatogram of the AR 73 solution at different electrolysis times during the electrochemical degradation process on Ti/SnO_2-Sb-CNT. a (0, 10, 20, and 30 min); (b) (0, 30, 90, and 180 min). Conditions: current density 50 mA cm^{-2}, initial concentration 1 g L^{-1}, pH (not adjusted), supporting electrolyte 0.1 M Na_2SO_4.

periods (0, 10, 20, and 30). According to the major peak at the retention time of 2.9 min, it was observed that AR 73 underwent remarkably efficient degradation by electrochemical oxidation on the anode, and the removal reached about 96% after 180 min. In the meantime, a group of intermediates with retention time from 2 to 2.4 min were detected at 30 min, and then the peaks decreased gradually along with AR 73 as the reaction time was extended and diminished at 180 min. Hence, although some intermediates were formed in the process of degradation, all of the organics could be removed by the Ti/SnO_2-Sn-CNT electrode.

4. Conclusions

In this study, electrochemical oxidation using the Ti/SnO_2-Sb-CNT anode indicates to be an attractive alternative for the degradation of AR 73. The cyclic voltammetric studies have revealed that the AR 73 is oxidized by indirect electrochemical oxidation, rather than direct electron transfer. The kinetic studies demonstrate the electrochemical oxidation of AR 73 obey the pseudo-first-order reaction kinetics. Under the experimental conditions, the degradation efficiency of AR 73 increases with increased current density, and the initial concentration of dye has the opposite effect. Besides, the initial pH value does not have obvious influence on the rate of degradation. The indirect electrochemical oxidation mediated by active chlorine using NaCl as supporting electrolyte contributes the dye degradation rate, but has poor effect on TOC removal efficiency due to the formation of refractory chlorinated compounds. Meanwhile, the electrogenerated oxidant plays a relative important role for degradation and mineralization. The performance of the three kinds of supporting electrolyte for AR 73 degradation in terms of mineralization efficiency is in order $Na_2SO_4 > Na_3PO_4 > NaCl$. The UV–vis spectra and HPLC analyses indicate that the AR 73 and intermediate products are completely eliminated after 3 h electrochemical degradation. The detailed mechanisms involved in the AR 73 degradation process need much deeper research in our following work, in order to provide more worthy information for industrial application of electrochemical degradation.

Acknowledgment

Our research was supported by the National Natural Science Foundation of China (grant number 21276177).

References

[1] C. O'Neill, F.R. Hawkes, D.L. Hawkes, N.D. Lourenço, H.M. Pinheiro, W. Delée, Colour in textile effluents–sources, measurement, discharge consents and simulation: A review, J. Chem. Technol. Biotechnol. 74 (1999) 1009–1018.

[2] A.B. dos Santos, F.J. Cervantes, J.B. van Lier, Review paper on current technologies for decolourisation of textile wastewaters: Perspectives for anaerobic biotechnology, Bioresour. Technol. 98 (2007) 2369–2385.

[3] S. Popli, U.D. Patel, Destruction of azo dyes by anaerobic–aerobic sequential biological treatment: A review, Int. J. Environ. Sci. 12 (2014) 1–16.

[4] J. Niu, Y. Bao, Y. Li, Z. Chai, Electrochemical mineralization of pentachlorophenol (PCP) by Ti/SnO_2-Sb electrodes, Chemosphere 92 (2013) 1571–1577.

[5] H. Lin, J. Niu, J. Xu, H. Huang, D. Li, Z. Yue, C. Feng, Highly efficient and mild electrochemical mineralization of long-chain perfluorocarboxylic acids (C9-C10) by Ti/SnO_2-Sb-Ce, Ti/SnO_2-Sb/Ce-PbO_2, and Ti/BDD electrodes, Environ. Sci. Technol. 47 (2013) 13039–13046.

[6] H. Lin, J. Niu, S. Ding, L. Zhang, Electrochemical degradation of perfluorooctanoic acid (PFOA) by Ti/SnO_2-Sb, Ti/SnO_2-Sb/PbO_2 and Ti/SnO_2-Sb/MnO_2 anodes, Water Res. 46 (2012) 2281–2289.

[7] F.J. Cervantes, A.B. Dos Santos, Reduction of azo dyes by anaerobic bacteria: microbiological and biochemical aspects, Rev. Environ. Sci. Biotechnol. 10 (2011) 125–137.

[8] L. Pereira, A.V. Coelho, C.A. Viegas, M.M. Santos, M.P. Robalo, L.O. Martins, Enzymatic biotransformation of the azo dye Sudan Orange G with bacterial cotA-laccase, J. Biotechnol. 139 (2009) 68–77.

[9] R. Jain, V. Gupta, S. Sikarwar, Adsorption and desorption studies on hazardous dye Naphthol Yellow S, J. Hazard. Mater. 182 (2010) 749–756.

[10] A. Aouni, C. Fersi, B. Cuartas-Uribe, A. Bes-Pía, M. Alcaina-Miranda, M. Dhahbi, Reactive dyes rejection and textile effluent treatment study using ultrafiltration and nanofiltration processes, Desalination 297 (2012) 87–96.

[11] M. Gao, Z. Zeng, B. Sun, H. Zou, J. Chen, L. Shao, Ozonation of azo dye Acid Red 14 in a microporous tube-in-tube microchannel reactor: Decolorization and mechanism, Chemosphere 89 (2012) 190–197.

[12] M.S. Lucas, A.A. Dias, A. Sampaio, C. Amaral, J.A. Peres, Degradation of a textile reactive azo dye by a combined chemical–biological process: Fenton's reagent-yeast, Water Res. 41 (2007) 1103–1109.

[13] A. del Río, J. Fernández, J. Molina, J. Bonastre, F. Cases, On the behaviour of doped SnO_2 anodes stabilized with platinum in the electrochemical degradation of reactive dyes, Electrochim. Acta 55 (2010) 7282–7289.

[14] U. Akpan, B. Hameed, Parameters affecting the photocatalytic degradation of dyes using TiO_2-based photocatalysts: A review, J. Hazard. Mater. 170 (2009) 520–529.

[15] C.A. Martínez-Huitle, E. Brillas, Decontamination of wastewaters containing synthetic organic dyes by electrochemical methods: A general review, Appl. Catal., B 87 (2009) 105–145.

[16] L.S. Andrade, T.T. Tasso, D.L. da Silva, R.C. Rocha-Filho, N. Bocchi, S.R. Biaggio, On the performances of lead dioxide and boron-doped diamond electrodes in the anodic oxidation of simulated wastewater containing the Reactive Orange 16 dye, Electrochim. Acta 54 (2009) 2024–2030.
[17] E. Guinea, J.A. Garrido, R.M. Rodríguez, P.-L. Cabot, C. Arias, F. Centellas, E. Brillas, Degradation of the fluoroquinolone enrofloxacin by electrochemical advanced oxidation processes based on hydrogen peroxide electrogeneration, Electrochim. Acta 55 (2010) 2101–2115.
[18] J.M. Aquino, G.F. Pereira, R.C. Rocha-Filho, N. Bocchi, S.R. Biaggio, Electrochemical degradation of a real textile effluent using boron-doped diamond or β-PbO_2 as anode, J. Hazard. Mater. 192 (2011) 1275–1282.
[19] M. Panizza, G. Cerisola, Direct and mediated anodic oxidation of organic pollutants, Chem. Rev. 109 (2009) 6541–6569.
[20] R.A. Torres, W. Torres, P. Peringer, C. Pulgarin, Electrochemical degradation of p-substituted phenols of industrial interest on Pt electrodes. Attempt of a structure–reactivity relationship assessment, Chemosphere 50 (2003) 97–104.
[21] C. Berríos, R. Arce, M. Rezende, M. Ureta-Zañartu, C. Gutiérrez, Electrooxidation of chlorophenols at a glassy carbon electrode in a pH 11 buffer, Electrochim. Acta 53 (2008) 2768–2775.
[22] K. Radha, V. Sridevi, K. Kalaivani, Electrochemical oxidation for the treatment of textile industry wastewater, Bioresour. Technol. 100 (2009) 987–990.
[23] S. Song, L. Zhan, Z. He, L. Lin, J. Tu, Z. Zhang, J. Chen, L. Xu, Mechanism of the anodic oxidation of 4-chloro-3-methyl phenol in aqueous solution using Ti/SnO_2-Sb/PbO_2 electrodes, J. Hazard. Mater. 175 (2010) 614–621.
[24] Y. Liu, H. Liu, J. Ma, J. Li, Investigation on electrochemical properties of cerium doped lead dioxide anode and application for elimination of nitrophenol, Electrochim. Acta 56 (2011) 1352–1360.
[25] S. Chai, G. Zhao, Y. Wang, Y.-N. Zhang, Y. Wang, Y. Jin, X. Huang, Fabrication and enhanced electrocatalytic activity of 3D highly ordered macroporous PbO_2 electrode for recalcitrant pollutant incineration, Appl. Catal., B 147 (2014) 275–286.
[26] X. Chen, P. Yao, D. Wang, X. Wu, Antimony and cerium co-doped tin oxide electrodes for pollutant degradation, Chem. Eng. J. 147 (2009) 412–415.
[27] T. Wu, G. Zhao, Y. Lei, P. Li, Distinctive tin dioxide anode fabricated by pulse electrodeposition: High oxygen evolution potential and efficient electrochemical degradation of fluorobenzene, J. Phys. Chem. C 115 (2011) 3888–3898.
[28] J. Wei, Y. Feng, X. Sun, J. Liu, L. Zhu, Effectiveness and pathways of electrochemical degradation of pretilachlor herbicides, J. Hazard. Mater. 189 (2011) 84–91.
[29] S.Y. Yang, Y.S. Choo, S. Kim, S.K. Lim, J. Lee, H. Park, Boosting the electrocatalytic activities of SnO_2 electrodes for remediation of aqueous pollutants by doping with various metals, Appl. Catal., B 111–112 (2012) 317–325.
[30] Y.-H. Cui, Y.-J. Feng, J. Liu, N. Ren, Comparison of various organic compounds destruction on rare earths doped Ti/Sb-SnO_2 electrodes, J. Hazard. Mater. 239–240 (2012) 225–232.
[31] W. Cheng, M. Yang, Y. Xie, B. Liang, Z. Fang, E.P. Tsang, Enhancement of mineralization of metronidazole by the electro-Fenton process with a Ce/SnO_2-Sb coated titanium anode, Chem. Eng. J. 220 (2013) 214–220.
[32] M. Panizza, G. Cerisola, Application of diamond electrodes to electrochemical processes, Electrochim. Acta 51 (2005) 191–199.
[33] M. Murugananthan, S. Yoshihara, T. Rakuma, N. Uehara, T. Shirakashi, Electrochemical degradation of 17β-estradiol (E2) at boron-doped diamond (Si/BDD) thin film electrode, Electrochim. Acta 52 (2007) 3242–3249.
[34] C.R. Costa, F. Montilla, E. Morallón, P. Olivi, Electrochemical oxidation of acid black 210 dye on the boron-doped diamond electrode in the presence of phosphate ions: Effect of current density, pH, and chloride ions, Electrochim. Acta 54 (2009) 7048–7055.
[35] L. Zhang, L. Xu, J. He, J. Zhang, Preparation of Ti/SnO_2-Sb electrodes modified by carbon nanotube for anodic oxidation of dye wastewater and combination with nanofiltration, Electrochim. Acta 117 (2014) 192–201.
[36] J.M. Aquino, R.C. Rocha-Filho, M.A. Rodrigo, C. Sáez, P. Cañizares, Electrochemical degradation of the reactive red 141 dye using a boron-doped diamond anode, Water Air Soil Pollut. 224 (2013) 1–10.
[37] C. Ramírez, A. Saldaña, B. Hernández, R. Acero, R. Guerra, S. Garcia-Segura, E. Brillas, J.M. Peralta-Hernández, Electrochemical oxidation of methyl orange azo dye at pilot flow plant using BDD technology, J. Ind. Eng. Chem. 19 (2013) 571–579.
[38] S.Y. Lee, G.A. Gagnon, Review of the factors relevant to the design and operation of an electrocoagulation system for wastewater treatment, Environ. Rev. 22 (2014) 421–429.
[39] V. Santos, Electrochemical degradation of azo dyes on BDD: Effect of chemical structure and operating conditions on the combustion efficiency, J. Environ. Eng. Manage. 18 (2008) 193–204.
[40] L. Xu, Z. Guo, L. Du, J. He, Decolourization and degradation of C.I. acid red 73 by anodic oxidation and the synergy technology of anodic oxidation coupling nanofiltration, Electrochim. Acta 97 (2013) 150–159.
[41] L. Xu, Z. Guo, L. Du, Anodic oxidation of azo dye C.I. Acid Red 73 by the yttrium-doped Ti/SnO_2-Sb electrodes, Front. Chem. Sci. Eng. 7 (2013) 338–346.
[42] Y.-H. Cui, Y.-J. Feng, Z.-Q. Liu, Influence of rare earths doping on the structure and electro-catalytic performance of Ti/Sb-SnO_2 electrodes, Electrochim. Acta 54 (2009) 4903–4909.
[43] R.J. Watts, M.S. Wyeth, D.D. Finn, A.L. Teel, Optimization of Ti/SnO_2-Sb_2O_5 anode preparation for electrochemical oxidation of organic contaminants in water and wastewater, J. Appl. Electrochem. 38 (2008) 31–37.
[44] N.B. Tahar, R. Abdelhédi, A. Savall, Electrochemical polymerisation of phenol in aqueous solution on a Ta/PbO_2 anode, J. Appl. Electrochem. 39 (2009) 663–669.

[45] R. Balzer, H. Vogt, Effect of electrolyte flow on the bubble coverage of vertical gas-evolving electrodes, J. Electrochem. Soc. 150 (2003) E11–E16.

[46] H. Lin, J. Niu, J. Xu, Y. Li, Y. Pan, Electrochemical mineralization of sulfamethoxazole by Ti/SnO_2-Sb/Ce-PbO_2 anode: Kinetics, reaction pathways, and energy cost evolution, Electrochim. Acta 97 (2013) 167–174.

[47] S. Song, J. Fan, Z. He, L. Zhan, Z. Liu, J. Chen, X. Xu, Electrochemical degradation of azo dye C.I. Reactive Red 195 by anodic oxidation on Ti/SnO_2-Sb/PbO_2 electrodes, Electrochim. Acta 55 (2010) 3606–3613.

[48] S. Yoshihara, M. Murugananthan, Decomposition of various endocrine-disrupting chemicals at boron-doped diamond electrode, Electrochim. Acta 54 (2009) 2031–2038.

[49] N. Borràs, R. Oliver, C. Arias, E. Brillas, Degradation of atrazine by electrochemical advanced oxidation processes using a boron-doped diamond anode, J. Phys. Chem. A 114 (2010) 6613–6621.

[50] Y. Samet, S.C. Elaoud, S. Ammar, R. Abdelhedi, Electrochemical degradation of 4-chloroguaiacol for wastewater treatment using PbO_2 anodes, J. Hazard. Mater. 138 (2006) 614–619.

[51] S. Garcia-Segura, E. Brillas, Mineralization of the recalcitrant oxalic and oxamic acids by electrochemical advanced oxidation processes using a boron-doped diamond anode, Water Res. 45 (2011) 2975–2984.

[52] C. Zhang, L. Liu, J. Wang, F. Rong, D. Fu, Electrochemical degradation of ethidium bromide using boron-doped diamond electrode, Sep. Purif. Technol. 107 (2013) 91–101.

[53] U. Schümann, P. Gründler, Electrochemical degradation of organic substances at PbO_2 anodes: Monitoring by continuous CO_2 measurements, Water Res. 32 (1998) 2835–2842.

[54] H. Li, J. Ni, Electrogeneration of disinfection byproducts at a boron-doped diamond anode with resorcinol as a model substance, Electrochim. Acta 69 (2012) 268–274.

[55] A. Wang, J. Qu, J. Ru, H. Liu, J. Ge, Mineralization of an azo dye Acid Red 14 by electro-Fenton's reagent using an activated carbon fiber cathode, Dyes Pigm. 65 (2005) 227–233.

[56] M. Stylidi, D.I. Kondarides, X.E. Verykios, Pathways of solar light-induced photocatalytic degradation of azo dyes in aqueous TiO_2 suspensions, Appl. Catal., B 40 (2003) 271–286.